# Influence of bridging atom in coppor-based coordination polymers for enhancing urease inhibition activity

Ling-Li Wang[a, c], Kai-Tong Wang[b], Wen-Long Duan*[b], Jian Luan*[b], Xiao-Ri Han*[a]

[a] *College of land and Environment, Shenyang Agricultural University, Shenyang, 110866, P. R. China*

[b] *College of Sciences, Shenyang University of Chemical Technology, Shenyang, 110142, P. R. China*

[c] *Institute of Applied Ecology, Chinese Academy of Sciences. Shenyang, 110016, P. R. China*

Emails: hanxr@syau.edu.cn; wlduan@syuct.edu.cn; 2010044@stu.neu.edu.cn

**Table S1** Crystallographic data for **Cu-CP-1** and **Cu-CP-2**.

| Cu-CP | **1** | **2** |
|---|---|---|
| Empirical formula | $C_{49}H_{55}ClCu_2N_8O_{16}$ | $C_{30}H_{24}Cu_3N_4O_{12}$ |
| $F_w$ | 1174.54 | 823.15 |
| Crystal system | Monoclinic | Triclinic |
| Space group | *C*2/*c* | *P*–1 |
| a (Å) | 14.4011(8) | 8.3526(10) |
| b (Å) | 16.9452(8) | 8.6543(10) |
| c (Å) | 22.2478(12) | 10.7547(13) |
| $\alpha$ (°) | 90 | 85.213(2) |
| $\beta$ (°) | 101.857(2) | 75.719(2) |
| $\gamma$ (°) | 90 | 80.446(2) |
| $V$ (Å$^3$), Z, $T$ (K) | 5313.3(5), 4, 296(2) | 742.20(15), 1, 296(2) |
| $D_c$/g cm$^{-3}$, F(000) | 1.468, 2432 | 1.842, 415 |
| Goodness-of-fit on $F^2$ | 1.030 | 1.019 |
| Reflections collected | 42125 | 3804 |
| Unique data, $R_{int}$ | 6977, 0.0495 | 2586, 0.0107 |
| $\theta$ Range (°) | 2.23–28.92 | 1.96–25.00 |
| $R_1$ ($I > 2\sigma(I)$)[a] | 0.0437 | 0.0296 |
| $wR_2$[b] (all data)[a] | 0.1256 | 0.0842 |

[a] $R_1 = \Sigma||F_o|-|F_c||/\Sigma|F_o|$, [b] $wR_2 = \Sigma[w(F_o^2-F_c^2)^2]/\Sigma[w(F_o^2)^2]^{1/2}$.

**Table S2** Selected bond distances (Å) and angles (°) for Cu-CP-**1**.

| | | | |
|---|---|---|---|
| Cu(1)–O(3) | 1.9646(16) | Cu(1)–O(1) | 1.9850(17) |
| Cu(1)–N(1) | 2.025(2) | Cu(1)–N(2) | 2.055(2) |
| Cu(1)–Cl(1) | 2.5447(7) | O(3)–Cu(1)–O(1) | 159.83(8) |
| O(3)–Cu(1)–N(1) | 89.05(8) | O(1)–Cu(1)–N(1) | 87.76(8) |
| O(3)–Cu(1)–N(2) | 90.64(7) | O(1)–Cu(1)–N(2) | 90.56(7) |
| N(1)–Cu(1)–N(2) | 174.25(8) | O(3)–Cu(1)–Cl(1) | 111.19(6) |
| O(1)–Cu(1)–Cl(1) | 88.96(6) | N(1)–Cu(1)–Cl(1) | 95.81(6) |
| N(2)–Cu(1)–Cl(1) | 89.65(6) | | |

**Table S3** Selected bond distances (Å) and angles (°) for Cu-CP-**2**.

| | | | |
|---|---|---|---|
| Cu(1)–O(6) | 1.892(2) | Cu(1)–O(6)#1 | 1.892(2) |
| Cu(1)–O(1)#1 | 1.940(2) | Cu(1)–O(1) | 1.940(2) |
| N(1)–Cu(2) | 2.069(2) | Cu(2)–O(6) | 1.880(2) |
| Cu(2)–O(3)#2 | 1.9641(19) | Cu(2)–O(2) | 1.972(2) |
| O(6)–Cu(1)–O(6)#1 | 180 | O(6)–Cu(1)–O(1)#1 | 86.95(9) |
| O(6)#1–Cu(1)–O(1)#1 | 93.05(9) | O(6)–Cu(1)–O(1) | 93.05(9) |
| O(6)#1–Cu(1)–O(1) | 86.94(9) | O(1)#1–Cu(1)–O(1) | 180 |
| O(6)–Cu(2)–O(3)#2 | 95.65(9) | O(6)–Cu(2)–O(2) | 89.56(8) |
| O(3)#2–Cu(2)–O(2) | 161.52(10) | O(6)–Cu(2)–N(1) | 177.11(9) |
| O(3)#2–Cu(2)–N(1) | 86.62(8) | O(2)–Cu(2)–N(1) | 87.74(9) |

Symmetry codes: #1 $-x + 1, -y, -z$; #2 $-x + 2, -y, -z$.

**Table S4** Hydrogen bonding geometries (Å, °) of Cu-CP-**1**.

| Cu-CP | D–H···A | D–H | H···A | D···A | D–H···A |
|---|---|---|---|---|---|
| **1** | N4–H4A···O2$^{i}$ | 0.86 | 2.10 | 2.8908 | 153 |

Symmetry code: $^{i}$ $1/2 - x, -1/2 + y, 1/2 - z$.

**Table S5** Comparison of inhibition of urease by the Cu-CPs and other materials.

| Materials | Percentage inhibition rate (100 μM)[a] | $IC_{50}$ ± SEM (μM) (3h)[b] | Reference |
|---|---|---|---|
| $Cu^{2+}$ | 87.50% | — | S1 |
| 3-dpye | — | — | — |
| HBCA | — | — | — |
| 1,2-$H_2$BDC | — | — | — |
| DMSO | — | — | — |
| AHA | 84.30% | 37.20 ± 4.00 | S2 |
| $[2HL]^{2+}\cdot[CuCl_4]^{2-}$ L = $N^1$,$N^1$,$N^2$,$N^2$-tetrakis(2-fluorobenzyl)ethane-1,2-diamine | 96.70% | 1.87 ± 0.01 | S3 |
| $[Cu(Hpz)_4Cl_2]$ Hpz = pyrazole | 99.70% | 0.93 ± 0.01 | S4 |
| tetrakis(m-bromo)-bis(m-4-chloro-2-((2-(piper idin-1-yl)ethyl)carbonoimidoyl)phenolato)-tri-copper(II) | — | 1.00 | S5 |
| $Cu(C_{19}H_{16}NO_2)_2$ | — | 1.45 | S6 |
| **Cu-CP-1** | 95.08 | 0.83 ± 0.01 | **This work** |
| **Cu-CP-2** | 90.96 | 2.53 ± 0.01 | **This work** |

[a] The concentration of the tested material is 100 μM.

[b] $IC_{50}$ values represent mean ± SD from three different experiments.

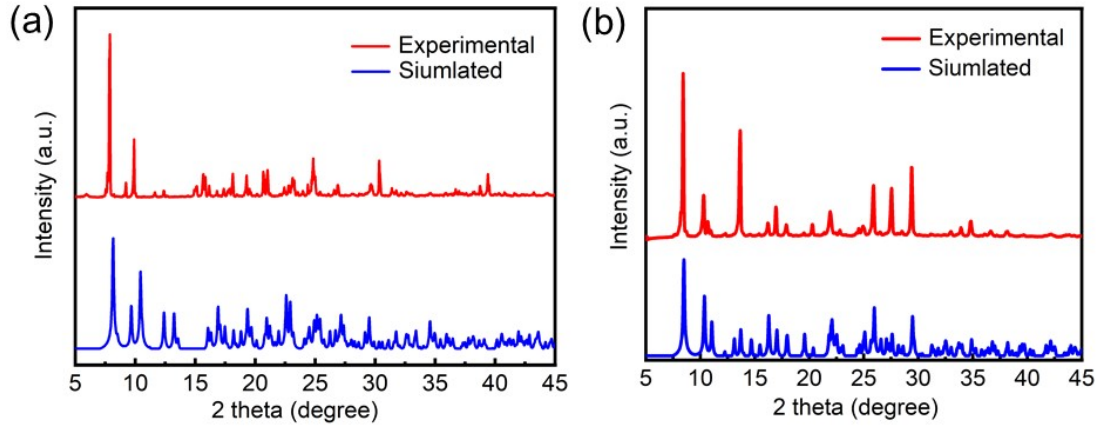


**Fig. S1** Experimental (red) and simulated (blue) PXRD patterns of Cu-CP-**1** (a) and Cu-CP-**2** (b).

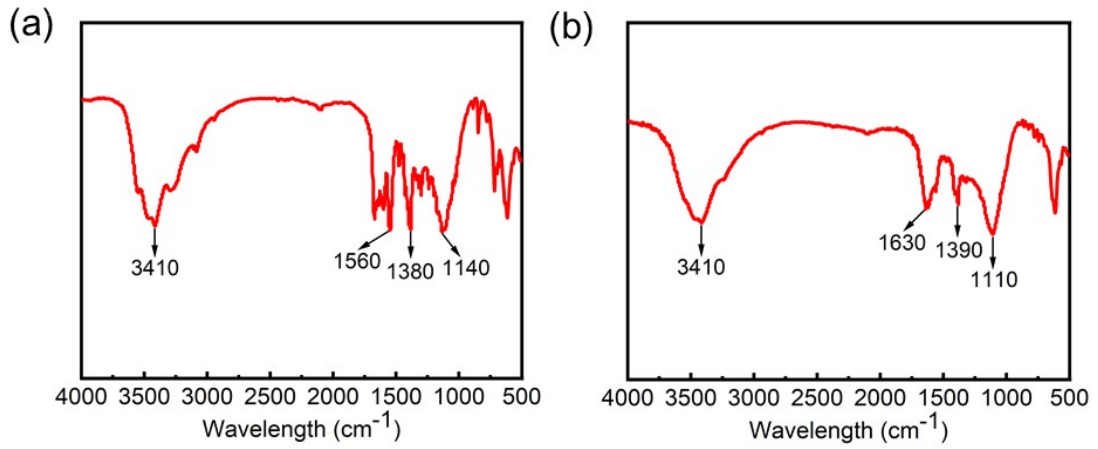


**Fig. S2** IR spectra of Cu-CP-**1** (a) and Cu-CP-**2** (b).

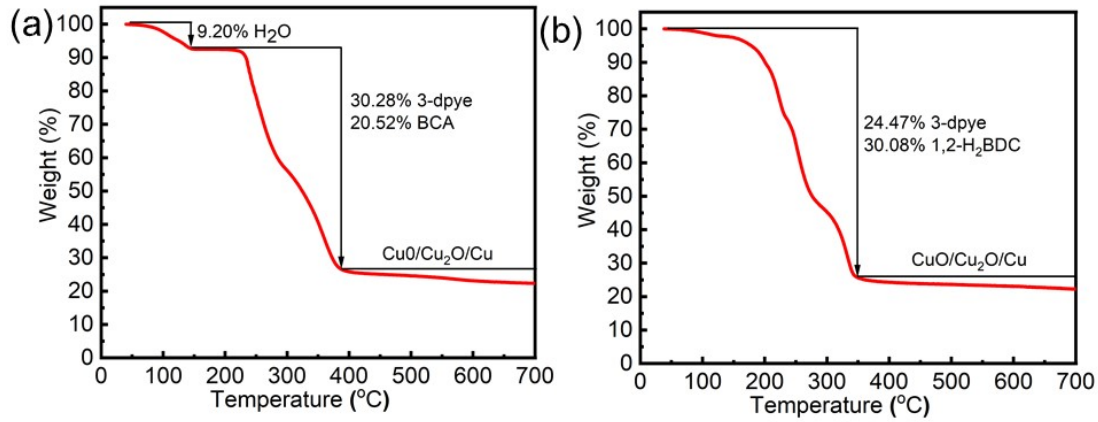


**Fig. S3** TGA curves of Cu-CP-**1** (a) and Cu-CP-**2** (b).

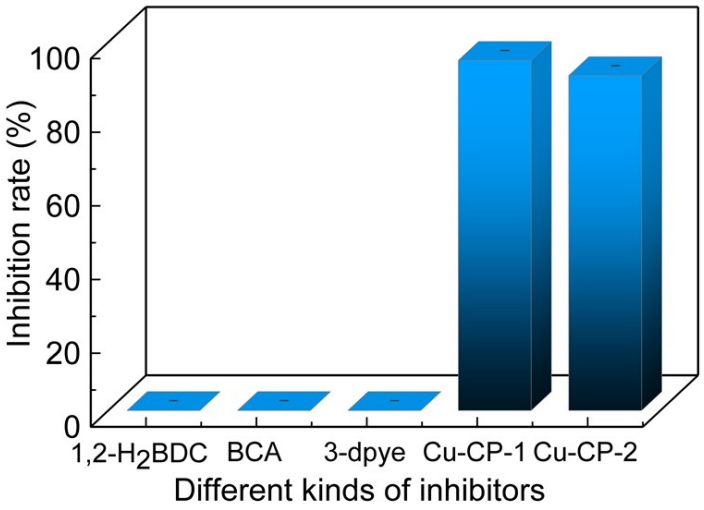


**Fig. S4** Different kinds of inhibitors

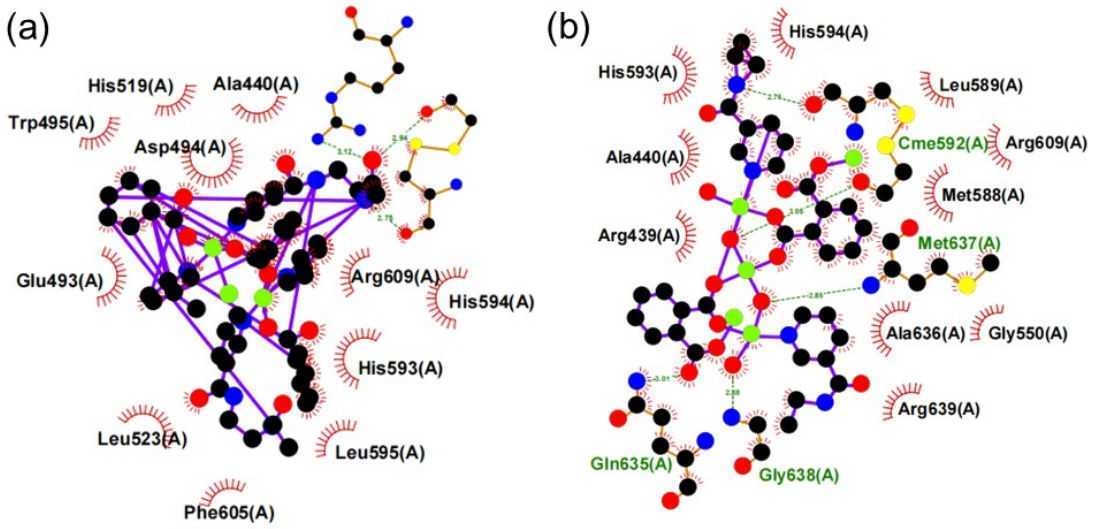


**Fig. S5** Binding mode of **Cu-CP-1** (a) and **Cu-CP-2** (b) with urease in 2D representation. Hydrogen bonds are presented as light dotted lines.

## References

S1 W. Chen, Y. G. Li, Y. M. Cui, X. Zhang, H. L. Zhu and Q. F. Zeng, *Eur. J. Med. Chem.*, 2010, **45**, 4473–4478.

S2 Z. L. You, M. Y. Liu, C. F. Wang, G. H. Sheng, X. L. Zhao, D. Qu and F. Niu, *RSC Adv.*, 2016, **6**, 16679–16690.

S3 W. L. Duan, C. Ma, J. Luan, F. Ding, F. Yan, L. Zhang and W. Z. Li, *Dalton Trans.*, 2023, **52**, 14329–14337.

S4 Y. X. Li, W. L. Duan, X. T. Zhai, J. Luan and F. Guo, *Inorg. Chim. Acta*, 2022, **543**, 121184.

S5 X. X. Chen, C. Y. Wang, J. J. Fu, Z. W. Huang, Y. Y. Xu and S. Q. Wang, *Inorg. Chem. Commun.*, 2019, **99**, 70–76.

S6 X. W. Dong, Y. G. Li, Z. W. Li, Y. M. Cui and H. L. Zhu, J. Inorg. Biochem., 2012, 108, 22–29.